

# Magnetic imaging by x-ray holography using extended references

Thomas A. Duckworth,<sup>1,\*</sup> Feodor Ogrin,<sup>1</sup> Sarnjeet S. Dhesi,<sup>2</sup>  
Sean Langridge,<sup>3</sup> Amy Whiteside,<sup>4</sup> Thomas Moore,<sup>4</sup>  
Guillaume Beutier,<sup>5</sup> and Gerrit van der Laan<sup>2</sup>

<sup>1</sup>*School of Physics and Engineering, University of Exeter, Stocker Road, Exeter EX4 4QL, UK*

<sup>2</sup>*Diamond Light Source, Harwell Science and Innovation Campus, Didcot OX11 0DE, UK*

<sup>3</sup>*ISIS, Science and Technology Facilities Council, Rutherford Appleton Laboratory, Didcot OX11 0QX, UK*

<sup>4</sup>*School of Physics and Astronomy, E. C. Stoner Laboratory, University of Leeds, Leeds LS2 9JT, UK*

<sup>5</sup>*SIMaP Grenoble-INP, CNRS, UJF, BP 75, 38402 Saint Martin D'Hères, France*

[\\*tad203@ex.ac.uk](mailto:*tad203@ex.ac.uk)

**Abstract:** We demonstrate magnetic lensless imaging by Fourier transform holography using extended references. A narrow slit milled through an opaque gold mask is used as a holographic reference and magnetic contrast is obtained by x-ray magnetic circular dichroism. We present images of magnetic domains in a Co/Pt multilayer thin film with perpendicular magnetic anisotropy. This technique holds advantages over standard Fourier transform holography, where small holes are used to define the reference beam. An increased intensity through the extended reference reduces the counting time to record the farfield diffraction pattern. Additionally it was found that manufacturing narrow slits is less technologically demanding than the same procedure for holes. We achieve a spatial resolution of  $\sim 30$  nm, which was found to be limited by the sample period of the chosen experimental setup.

© 2011 Optical Society of America

**OCIS codes:** (090.1995) Digital holography; (340.7440) X-ray imaging; (260.6048) Soft x-rays; (310.6870) Thin films, other properties.

---

## References and links

1. S. Eisebitt, J. Lüning, W. F. Schlotter, M. Lörger, O. Hellwig, W. Eberhardt, and J. Stöhr, "Lensless imaging of magnetic nanostructures by x-ray spectro-holography," *Nature* **432**, 885–888 (2004).
2. C. Tieg, R. Frömter, D. Stickler, S. Hankemeier, A. Kobs, S. Streit-Nierobisch, C. Gutt, G. Grübel, and H. P. Oepen, "Imaging the in-plane magnetization in a Co microstructure by Fourier transform holography," *Opt. Express* **18**, 27251–27256 (2010).
3. O. Hellwig, S. Eisebitt, W. Eberhardt, W. F. Schlotter, J. Lüning, and J. Stöhr, "Magnetic imaging with soft x-ray spectroholography," *J. Appl. Phys.* **99**, 08H307 (2006).
4. S. Streit-Nierobisch, D. Stickler, C. Gutt, L.-M. Stadler, H. Stillrich, C. Menk, R. Frömter, C. Tieg, O. Leupold, H. P. Oepen, and G. Grübel, "Magnetic soft x-ray holography study of focused ion beam-patterned Co/Pt multilayers," *J. Appl. Phys.* **106**, 083909 (2009).
5. C. Tieg, E. Jimenez, J. Camerero, J. Vogel, C. Arm, B. Rodmacq, E. Gautier, S. Auffert, B. Delaup, G. Gaudin, B. Dieny, and R. Miranda, "Imaging and quantifying perpendicular exchange biased systems by soft x-ray holography and spectroholography," *Appl. Phys. Lett.* **96**, 072503 (2010).
6. H. Hopster and H. P. Oepen, *Magnetic Microscopy of Nanostructures* (Springer, 2005).
7. S. G. Podorov, K. M. Pavlov, and D. M. Paganin, "A non-iterative reconstruction method for direct and unambiguous coherent diffractive imaging," *Opt. Express* **15**, 9954–9962 (2007).

8. M. Guizar-Sicairos and J. R. Fienup, "Holography with extended reference by autocorrelation linear differential operation," *Opt. Express* **15**, 17592–17612 (2007).
9. M. Guizar Sicairos and J. R. Fienup, "Direct image reconstruction from a Fourier intensity pattern using HERALDO," *Opt. Lett.* **33**, 2668–2670 (2008).
10. D. Zhu, M. Guizar-Sicairos, B. Wu, A. Scherz, Y. Acremann, T. Tyliczszak, P. Fischer, N. Friedenberger, K. Ollefs, M. Farle, J. R. Fienup, and J. Stöhr, "High-resolution x-ray lensless imaging by differential holographic encoding," *Phys. Rev. Lett.* **105**, 043901 (2010).
11. D. Gauthier, M. Guizar-Sicairos, X. Ge, W. Boutu, B. Carré, R. J. Fienup, and H. Merdji, "Single-shot femtosecond x-ray holography using extended references," *Phys. Rev. Lett.* **105**, 093901 (2010)
12. G. van der Laan and C. R. Physique, "Soft x-ray resonant magnetic scattering of magnetic nanostructures," **9**, 570–584 (2008).
13. G. Beutier, A. Marty, F. Livet, G. van der Laan, S. Stanesco, and P. Bencok, "Soft x-ray coherent scattering: instrument and methods at ESRF ID08," *Rev. Sci. Instrum.* **78**, 093901 (2007).
14. H. He, U. Weierstall, J. C. H. Spence, M. Howells, H. A. Padmore, S. Marchesini, and H. N. Chapman, "Use of extended and prepared reference objects in experimental Fourier transform x-ray holography," *Appl. Phys. Lett.* **85**, 2454–2456 (2004).
15. S. Eisebitt, M. Lörger, W. Eberhardt, J. Lüning, J. Stöhr, C. T. Rettner, O. Hellwig, E. E. Fullerton, and G. Denbeaux, "Polarization effects in coherent scattering from magnetic specimen: implications for x-ray holography, lensless imaging, and correlation spectroscopy," *Phys. Rev. B* **68**, 104419 (2003).
16. A. Scherz, W. F. Schlotter, K. Chen, R. Rick, J. Stöhr, J. Lüning, I. McNulty, Ch. Günther, F. Radu, W. Eberhardt, O. Hellwig, and S. Eisebitt, "Phase imaging of magnetic nanostructures using resonant soft x-ray holography," *Phys. Rev. B* **76**, 214410 (2007).
17. S. Hashimoto and Y. Ochiai, "Co/Pt and Co/Pd multilayers as magneto-optical recording materials," *J. Magn. Magn. Mater.* **88**, 211–226 (1990).
18. V. Baltz, A. Marty, B. Rodmacq, and B. Dieny, "Magnetic domain replication in interacting bilayers with out-of-plane anisotropy: Application to Co/Pt multilayers," *Phys. Rev. B* **75**, 014406 (2007)
19. A. Hubert and R. Schäfer, *Magnetic Domains: The Analysis of Magnetic Microstructures* (Springer Verlag, 1998).
20. W. F. Schlotter, R. Rick, K. Chen, A. Scherz, J. Stöhr, J. Lüning, S. Eisebitt, C. Gunther, W. Eberhardt, O. Hellwig, and I. McNulty, "Multiple reference Fourier transform holography with soft x rays," *Appl. Phys. Lett.* **89**, 163112 (2006).
21. J. R. Fienup, "Phase retrieval algorithms: a comparison," *Appl. Opt.* **21**, 2758–2769 (1982).

## 1. Introduction

Characterization of magnetic states on the submicron scale is a challenging task but holds promise for rapid advances in understanding and utilizing the properties of new materials for spintronic devices. Fourier transform holography (FTH) is a well established lensless technique for imaging the perpendicular component of magnetic domains [1] and more recently systems with in-plane magnetization [2]. Holographic imaging is suitable not only for the remanent state [1] [as typically performed in the case of, e.g. photoemission electron microscopy (PEEM) or magnetic force microscopy (MFM)], but can also be used under applied electric and magnetic fields [3–5] and shows great potential for studying the dynamics of multiferroic thin films. Like other photon-in photon-out techniques, x-ray holography offers the opportunity to follow the evolution of magnetic domain structures and to study the intrinsic properties of materials. Complementary to MFM or Lorentz microscopy [6], x-ray holography has the specific advantage of being sensitive to the three-dimensional magnetization profile. Furthermore, its element specificity is beneficial to the study of heterogeneous systems.

A recent development in the field of FTH has reduced the restrictions on the reference size to allow a much wider range of possibilities. The technique, known as holography with extended reference by autocorrelation linear differential operator (HERALDO) [7, 8], permits the use of larger objects as references without compromising the spatial resolution. Since its first experimental demonstration in 2008 [9], reports of HERALDO have revealed its lensless imaging capabilities in coherent soft x-ray scattering [10] and ultrafast single-shot imaging [11]. A comparison with other microscopy techniques, such as a full field transmission x-ray microscope (TXM) and a scanning transmission x-ray microscope (STXM), where high resolution zone plate optics are used, can be found in Zhu et al. [10]. Unlike standard FTH using holes

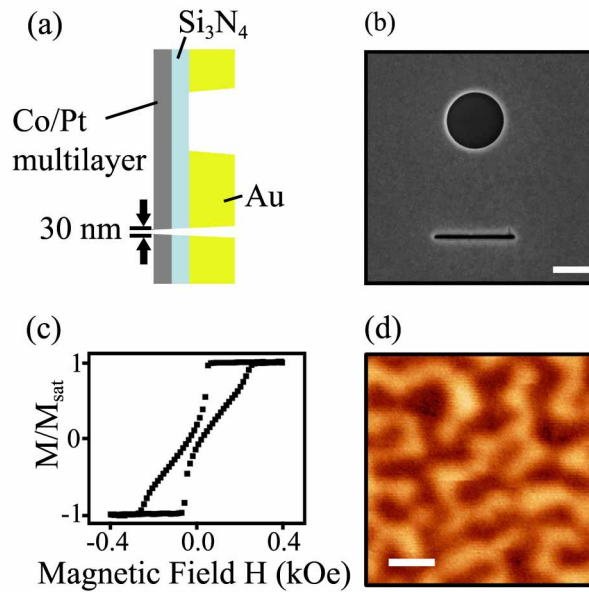


Fig. 1. (Color online) (a) Schematic of the sample design cross section. (b) Scanning Electron Micrograph (SEM) of the object aperture and the reference slit viewed from the side of the Au mask (scale bar = 1  $\mu\text{m}$ ). (c) Polar MOKE hysteresis loop of the Co/Pt multilayer. (d) Typical MFM image showing the maze domain structure that forms in a  $[\text{Co}(5\text{\AA})/\text{Pt}(10\text{\AA})]\times 30$  multilayer at remanence (scale bar = 300 nm).

as point references, in HERALDO the reference emerges from boundary waves produced by sharp corners or edges of an extended object. In principle, the highest resolution possible is no longer limited by the size of the reference, but rather by the quality of its sharpest features. In our experiment we have chosen an extended reference where boundary waves emerge from both edges of a narrow slit. The far-field diffraction pattern formed from the interference between the waves from the object and extended reference produces a hologram. The hologram is multiplied digitally with a differential filter, and after a simple Fourier transform of this result, a complex valued reconstruction is retrieved.

In this paper we demonstrate the use of HERALDO as a means of identifying the magnetic domain patterns which form in the remanent state of a Co/Pt multilayer film. A magnetic multilayer of  $[\text{Co}(5\text{\AA})/\text{Pt}(10\text{\AA})]\times 30$  was deposited onto the front side of a 100 nm thick Si<sub>3</sub>N<sub>4</sub> membrane. A 600 nm Au film was deposited on the reverse side of the membrane to form an x-ray opaque mask. Focused ion beam (FIB) milling was used to fabricate a reference slit ( $2\ \mu\text{m} \times 30\ \text{nm}$ ) and a viewing aperture ( $1.5\ \mu\text{m}$  diameter) in the mask. A schematic cross section through the sample is shown in Fig. 1(a), and a scanning electron micrograph of the viewing aperture and reference slit is shown in Fig. 1(b). The slit length and distance from the viewing aperture were chosen such that separation conditions [8] prevented real space objects in the reconstruction from overlapping.

## 2. Results and Discussion

The polar magneto-optical Kerr effect (MOKE) hysteresis loop for the Co/Pt multilayer film is shown in Fig. 1(c), which indicates that the sample possesses perpendicular magnetic

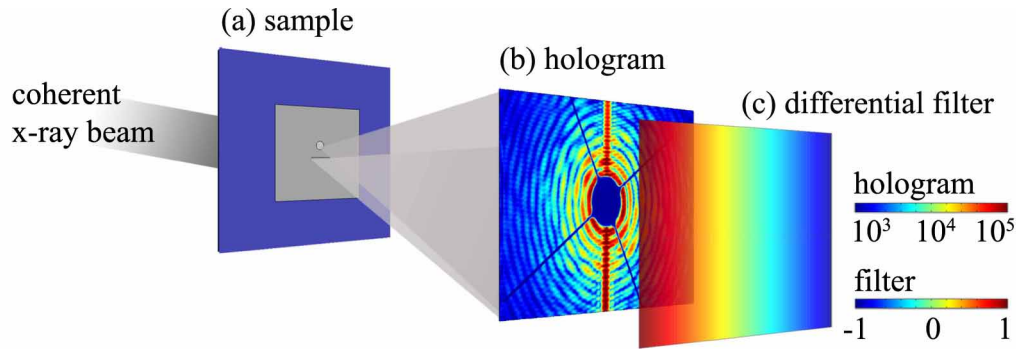


Fig. 2. (Color online) (a) The object and reference slit are illuminated by the coherent x-ray beam. (b) The hologram formed by the interference of the scattered x-rays from the object and reference slit is recorded on the CCD camera in the far field. (c) A linear differential filter, defined by the derivative of the slit direction, is multiplied by the hologram before performing a Fourier transform to retrieve the reconstructed image.

anisotropy. This is supported by the MFM image, shown in Fig. 1(d), which reveals the typical maze pattern of antiferromagnetically coupled up and down domains formed in the multilayer at remanence.

In our experiment we exploit x-ray magnetic circular dichroism (XMCD) to achieve magnetic contrast. The tunability of the energy and polarization of the x-rays from a synchrotron allows for an element-specific enhancement of the magnetic scattering [12]. Measurements were performed at the Co  $L_3$  absorption edge ( $h\nu=778$  eV or  $\lambda=15.9$  Å) using circularly polarized x-rays from beamline I06 at Diamond Light Source. The experimental set-up is depicted in Fig. 2. A pinhole, 20  $\mu\text{m}$  in diameter, was placed upstream from the sample [see Fig. 2 (a)] to skim the x-ray beam, extracting a small fraction with nearly full transverse coherence [13] and defining the spot size. Holograms were recorded using a charge-coupled device (CCD) camera (Princeton Instruments, 2048 $\times$ 2048 pixels of size 13.5  $\mu\text{m}$ ) placed 450 mm downstream from the sample. A beamstop, consisting of a  $\sim 600$   $\mu\text{m}$  diameter disk on two  $\sim 50$   $\mu\text{m}$  diameter crosswires, was used to block the direct x-rays and so prevent overexposure of the CCD.

A drawback of standard FTH is a low contrast of the interference fringes, particularly at larger scattering angles where the higher resolution information is encoded. The relative photon flux from the object and reference determines the fringe visibility. Improving the contrast typically compromises the spatial resolution as the reference would need to be enlarged to obtain a higher throughput [14]. This problem is significantly alleviated in HERALDO as the flux passing through the extended reference can be far greater than that of a reference hole. Apart from the pixel size and acceptance angle of the CCD, the ultimate resolution in the reconstruction is limited in the direction across the slit by the slit width, and along the slit, by the sharpness of the edges. Moreover, manufacture of extended objects proves to be less demanding than that of reference pinholes due to the nature of FIB milling [10]. Interestingly, we found that slits could be manufactured with a width smaller than the size of a reference hole. Upon analyzing the point spread function (PSF) of the two approaches, a reference hole gives a broader response than the derivative of a slit edge.

The differential filter to be multiplied to the hologram is defined by the directional derivative of the edges from the extended reference. Prior knowledge of the slit orientation is however not required as it is readily determined from the intense streak that it forms in the recorded holo-

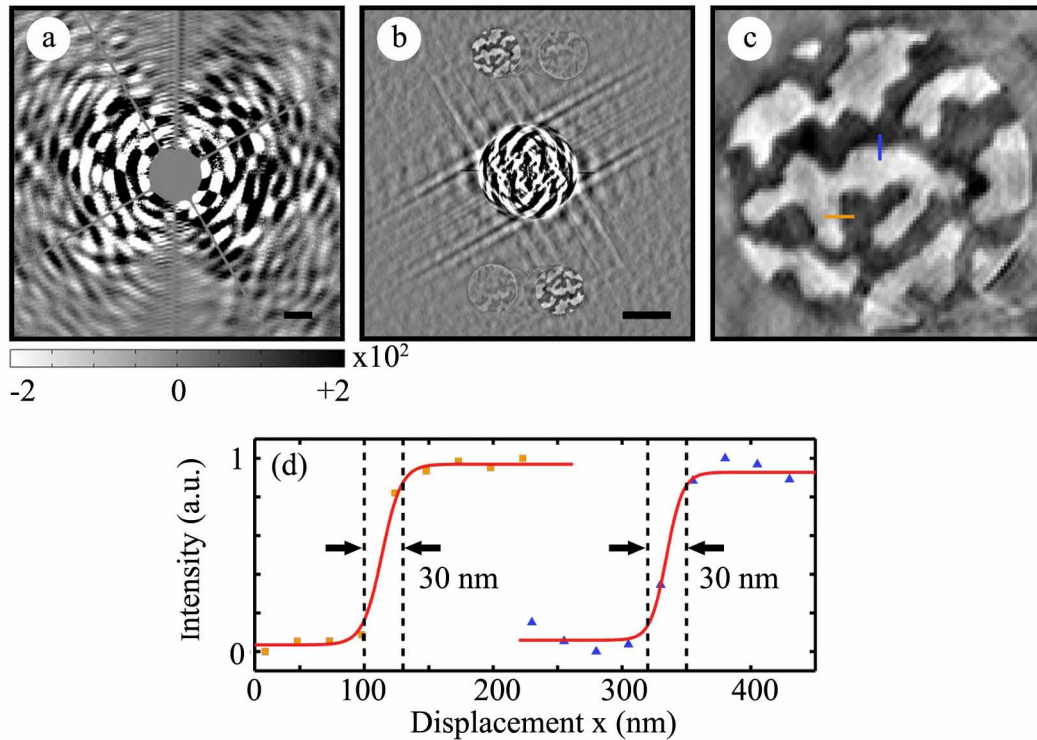


Fig. 3. (Color online) (a) Difference between the images taken with the two opposite x-ray helicities after applying a differential filter (only the central  $1000 \times 1000$  pixels are shown. Scale bar =  $20 \mu\text{m}^{-1}$ ). (b) Fourier transform of (a), showing the real part of the image. The crosscorrelations between the reference slit edges and the object, and their twin images can be seen (only the central  $410 \times 410$  pixels are shown. Scale bar =  $1.5 \mu\text{m}$ ). (c) Magnified view of one of the crosscorrelations from (b); the thin lines across the domains indicate the location where the profile scans in (d) were taken. (d) The horizontal line scan (orange square symbols) corresponds to the resolution along the slit direction. The intensity profile across the domain vertically (blue triangle symbols) corresponds to the resolution across the width of the slit. The data is fitted (red lines) using a hyperbolic tangent and the resolved width of the domain wall is obtained as  $w \approx 30 \pm 10 \text{ nm}$  in both directions. For clarity, both curves have been shifted arbitrarily along the  $x$ -axis.

gram, as can be seen in Fig. 2(b). Accumulations of 10 images, each frame with an exposure time of 40 s on the full area of the CCD, were recorded for the two opposite x-ray helicities under attenuated beam intensity. The difference between the images for the two helicities gives the magnetic contrast [15]. The 800 s total exposure time used to achieve the reconstruction should not be taken as being representative for the required image acquisition time, as we did not optimize this aspect of the measurement. The difference image multiplied by the differential filter [see Fig. 2(c)] is shown in Fig. 3(a) with the corresponding Fourier transform shown in Fig. 3(b). The reference provides a Dirac delta function at either end of the slit. This reconstruction reveals four object-reference crosscorrelations, which are two-by-two conjugated. Each conjugate image shows the same domain structure, similar to the case of traditional FTH. Also the image reconstructions at opposite ends of the slit display the same structure, but as seen in Fig. 3(b) they show an unexpected difference in contrast and reversal in color. The image reconstructions can indeed have different global amplitude and phase if the slit is not uniformly

illuminated. Whilst the origin of the color reversal remains less clear, it has been reported by Scherz et al. [16] that a phase change may arise from an inappropriate determination of the centre of symmetry, loss of high- $q$  information due to the limited size of the CCD, or loss of low- $q$  information due to the beamstop. The shadowing from the beamstop can be reduced by a simple modification of the design. Furthermore, faint rings can be seen in the reconstruction between the cross correlations which we believe are due to irregularities along the slit edge. We found that the magnetic domain structure in the images is completely reproducible with the same details observed after the sample had been removed and placed back in the set-up several weeks later.

Figure 3(c) shows an enlargement of the crosscorrelation image with the best contrast. The orthogonal lines in the image indicate where vertical and horizontal line scans were made across a domain wall, and these are plotted in Fig. 3(d). The resolution of the imaging can be estimated by taking into account the typical width of a domain wall in CoPt multilayer films ( $< 10$  nm) [16, 17]. By fitting the measured intensity profile with a hyperbolic tangent of the form  $I = I_0 \tanh[2(x - x_0)/w] + I_C$  [18], where  $x_0$  is the center position of the domain wall,  $w$  is its width and,  $I_0$  and  $I_C$  are intensity offset values, we obtain a width of the domain boundary  $w \approx 30 \pm 10$  nm in both directions. This value is of the order of the sample period ( $\sim 30$  nm), and is thus limited by the maximal acceptance angle of the CCD camera.

### 3. Conclusion

In conclusion we demonstrate holographic magnetic imaging using HERALDO. The total resolution achieved in our experimental set-up is limited by the sample period ( $\sim 30$  nm), which is larger than the physical domain wall width. Within the error bar, the resolution is the same in the vertical and horizontal direction (the latter corresponds to HERALDO filtering). Compared to the conventional FTH method, the clear benefits are expected to be found in a reduction of the image acquisition time, due to an increased intensity through the extended reference, and the easier manufacturing of reference slits compared to holes. The method as described here has significant scope for improvement and a resolution of  $\sim 15$  nm [10] seems to be achievable in the near future. Spatial multiplexing could be applied with additional extended references to improve the signal-to-noise ratio [20]. Furthermore, HERALDO is a non-iterative approach, which offers a fast and simple reconstruction method that could be used as the starting for further iterative phase retrieval algorithms [21]. The technique is robust, similar to previous FTH methods, and is equally suitable for imaging under extreme conditions, such as high magnetic fields or low temperatures. We recognize HERALDO as a promising approach for the future studies of magnetic systems. Its ability to directly image magnetic configurations within an applied field could greatly benefit the advance of magnetic logic devices and magnetic race track memory devices where understanding the propagation and controlled pinning of magnetic domain walls along nanowires is desired.

### Acknowledgments

The authors gratefully acknowledge the assistance of Paul S. Keatley with the polar MOKE measurements and thank the Centre for Material Physics and Chemistry (CMPC) of the Science and Technology Facilities Council (STFC), UK and the Engineering and Physical Sciences Research Council (EPSRC), UK for funding.